RP Materials: Proceedings
Vol. 1, Part 1 (2022) pp. 13–16
e-ISSN:

RESEARCH PLATEAU PUBLISHERS

Cite this article: H.P. Singh, Nonlinear absorption of ternary and quaternary semiconductor nanocrystals, *RP Materials: Proceedings* Vol. 1, Part 1 (2022) pp. 13–16.

**Original Research Article**

# Nonlinear absorption of ternary and quaternary semiconductor nanocrystals

**Harjit Pal Singh**
Department of Electronics and Communication Engineering, C.T. Group of Institutions,
Urban Estate Phase II, Partappura Road, Shahpur, Jalandhar - 144020, India
*Corresponding author, E-mail: hpalctgroup@gmail.com

****Selection and Peer-Review under responsibility of the Scientific Committee of the National Conference on Advanced Engineering Materials (NCAEM 2022).**

**ARTICLE HISTORY**
Received: 10 Aug. 2022
Revised: 12 Nov. 2022
Accepted: 13 Nov. 2022
Published online: 27 Dec. 2022

**KEYWORDS**
Nonlinear absorption; ternary/ quarternary semiconductor nanocrystals.

**ABSTRACT**
In this article, I discuss the nonlinear absorption characteristics of colloidal-synthesised semiconductor nanocrystals with varied bandgap sizes, such as CdSeS (ternary) and ZnCdSeS (quaternary), in the picosecond domain under both resonant and non-resonant electronic excitation. Using the conventional open aperture Z-scan technique, the nonlinear absorption was measured. The excitation sources were two wavelengths from a hybrid mode-locked Nd: YAG laser at (532 nm) the second harmonic and (1064 nm) the fundamental radiation, which produced 35 pico-second pulses with the repetition rate of 10 Hz. A 300 mm focal length lens was utilised to focus the input coherent radiation to the 40 µm spot size, and a photodiode was employed to gather the transmitted light. The focus' peak intensities vary between 2 - 40 $GWcm^{-2}$. For potential optical limiting and switching applications, the emergence of nonlinear absorption and its cross-section are investigated in ternary and quaternary nanocrystals.

## 1. Introduction

Due to quantum confinement, semiconductor nanocrystals (NCs) feature fascinating size- and shape-dependent optical and electrical properties [1]. Numerous optical nonlinearities and optoelectronic features of semiconductor NCs doped in glasses [2] and colloidal solutions [3, 4] have been investigated. When compared to their bulk counterparts, CdS, CdSe, and ZnS nanocrystals' nonlinear optical absorption in the colloids formation has been observed as many times higher [4-6]. Third order nonlinear susceptibilities were found to be 200% higher in CdSe/ZnS quantum dots [6] due to structural alterations like core/shell that caused surface passivation. The intrinsic energy states of an NC can change according on its size and form, which has a significant impact on its nonlinear characteristics. The crucial processes for exciting nonlinear absorption (NLA) behaviour in diverse nanostructures are two-photon absorption (2PA) and excited state absorption (ESA).

ESA dominates under the resonant electronic excitation circumstances $E_g \approx h\nu$, where $E_g$ represents the band gap energy and ν is frequency of the input photon. A nanostructure that would typically be activated by a single photon with a resonant wavelength is capable of simultaneously absorbing two or more photons of longer wavelength when non-resonant excitation circumstances ($E_g > h\nu$) are present. Because: (i) this is able to produce excited states when irradiated by photons having energy smaller than the necessary energy of excitation, and (ii) the intensity reliance of two-photon absorption makes it possible for a higher spatial selectivity in a system's excitation, the two-photon absorption process has attracted significant interest in a variety of applications. In comparison to resonant nonlinearities, non-resonant nonlinearities also have faster response times. Even in resonant excitation, materials with unique energy level structures exhibit two-photon absorption behaviour when exposed to high input irradiances [7, 8]. We discuss the nonlinear absorption characteristics of colloidal-synthesised CdSeS (ternary) and ZnCdSeS (quaternary) semiconductor NCs with various $E_g$ in the picosecond regime under resonant and non-resonant electronic stimulation. For prospective optical limiting and switching applications, the emergence of nonlinear absorption and its cross-section are investigated in ternary and quaternary NCs (TNCs and QNCs).

## 2. Materials and methods

The details of the colloidal approach used to manufacture the NCs are published elsewhere [9]. By adjusting the Se/S ratio, ZnCdSeS can be controlled throughout a variety of visible regions, while the band gap and associated band edge emission of CdSeS NCs were tuned across the whole visible region. The distinct existence of high quality, virtually monodisperse NCs is shown by the sharp initial excitonic absorption peak and narrow emission (FWHM 32 – 35 nm). HRTEM pictures are used to assess the NCs' sizes. The particles form a hexagonal close-packed array on the TEM grid and are extremely crystalline, displaying lattice fringes. More than 200 different nanocrystallites were carefully measured for size to get the size and size-distribution data. The ZnCdSeS NCs possess the mean particle dimensions of 6.6 nm and 6.4 nm with $E_g$ of 2.1 and 2.0 eV, respectively, while the TNCs

have the mean particle dimensions of 6.2 nm with 9% tolerance and $E_g$ of 2.05 and 2.26 eV. This results in a weak quantum confinement of electrons inside NCs. In Table 1, the NCs' size and $E_g$ are listed. The diameters of the NCs made with various Se/S ratios are comparable, proving that the alteration in the band gap of various NCs is essentially brought on by the alteration in elemental composition. The creation of a homogeneous alloyed structure and a perfect core/shell structure are excluded by photoelectron spectroscopy (PES) with different photon energy, but complicated structures with S content progressively rising relative to Se from the core towards the surface of the NCs are observed instead. The nonlinear absorption was studied with the use of the widely utilised Z-scan method [10]. The excitation sources were two wavelengths from a hybrid mode-locked Nd: YAG laser, the (532 nm) second harmonic and the (1064 nm) fundamental light, which produced pulses of 35 pico-second and the repetition rate of 10 Hz. A 300 mm focal length lens was utilised to focus the input coherent radiation to 40 µm spot size and a photodiode was employed to gather the transmitted light. The focus' peak intensities vary between 2 and 40 GWcm$^{-2}$.

## 3. Results and discussion

Both systems displayed intriguing nonlinear absorption behaviour with increasing input irradiance when subjected to resonant electrical excitation. We demonstrate saturable absorption (SA), or a rise in the normalised transmittance near focus, for the TNCs with $E_g$ of 2.26 eV, (CdSeS-II), at lower intensity (3.8 GWcm$^{-2}$) (Figure 1A). We observe abrupt drops in the normalised transmittance around Z = 0 with increasing input intensity (11.4 and 26.8 GWcm$^{-2}$), which are caused by reverse saturable absorption (RSA). With CdSeS-I, a similar pattern of behaviour is seen, and Figure 1B shows the Z-scan (open aperture) curve with RSA at an intensity of input radiation equal to 38.6 GWcm$^{-2}$. QNCs exhibit a comparable nonlinear absorption pattern, although at relatively lower input intensities (Figure 1C). In TNCs and QNCs, the RSA has been observed at input intensities of around 11 and 8 GWcm$^{-2}$, respectively. The transmission at Z = 0 for QNCs reaches up to 0.82 with an input of 15.3 GWcm$^{-2}$, showing the presence of higher nonlinear absorption. A decrease in transmission at greater input irradiance, in addition to linear absorption, suggests the inclusion of an intensity-dependent absorption channel [7, 8], and this transition from SA to RSA suggests fascinating excited state dynamics in these systems. Even at very low input intensities, these samples exhibit pure RSA behaviour under nonresonant excitation circumstances with 1064 nm (1.65 eV). At an input intensity of 3.95 GWcm$^{-2}$, Figure 1D's open aperture Z-scan curve for ZnCdSeS basically exhibits pure RSA behaviour. The theoretical fits achieved using the model described below have been depicted in figure.

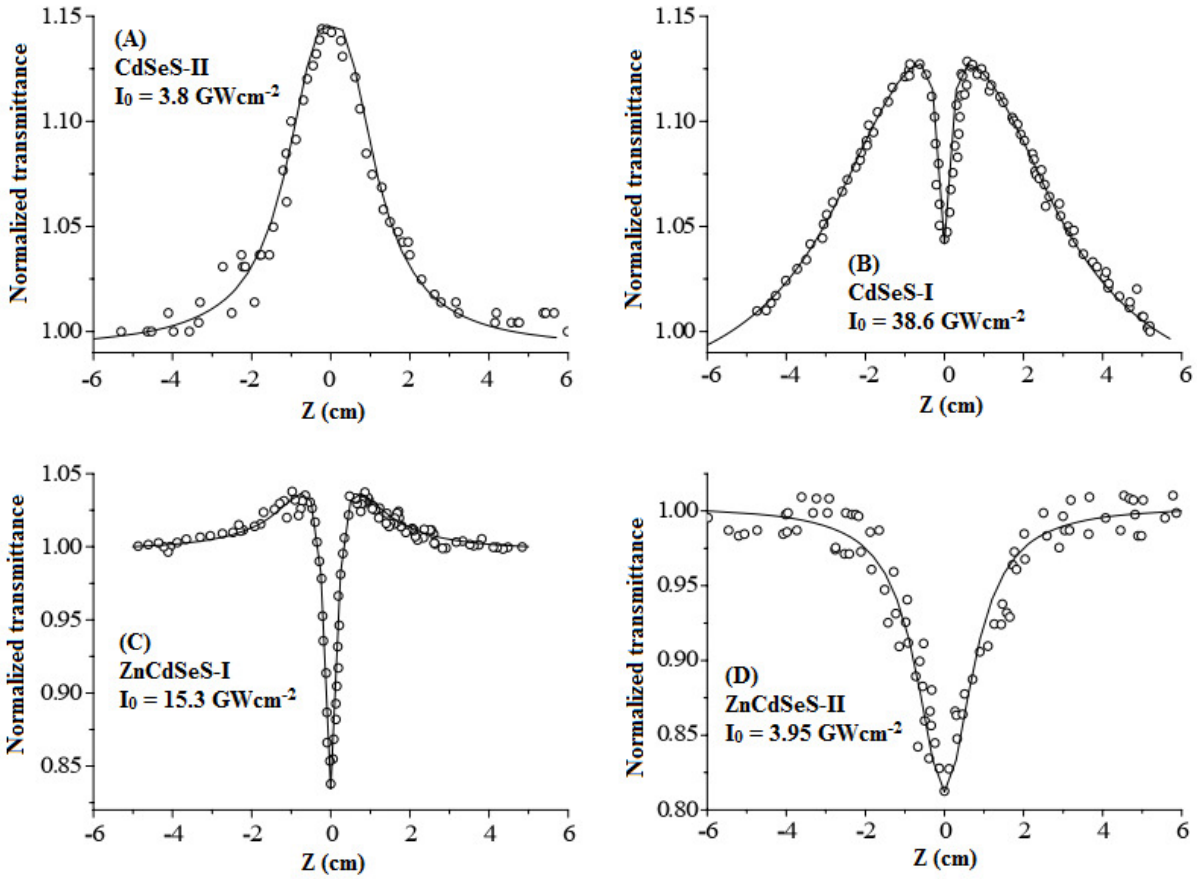


**Figure 1:** Z-scan (open aperture) curves for TNCs and QNCs at various input intensities under resonant (A–C) and nonresonant (D) excitation circumstances.

As the HOMO-LUMO gap of these NCs is smaller than the excitation energy of 2.33 eV (532 nm), the input photon excites an electron via one-photon interband absorption. A typical recombination time later, the excited electron recombines radiatively with a hole after first decaying non-radiatively to the LUMO via coupling to lattice vibrations. The photoluminescence (PL) lifetime, which is non-radiative, occurs throughout picosecond time scales and has a typical lifetime of nanoseconds [1]. There is a good chance that two distinct excitations will take place with a high enough input irradiance. Both scenarios result in a dip around Z = 0: in the first, the excited electron may absorb an additional photon, causing an intraband excited state absorption (ESA) from the lower to higher electronic states, and in the second, an interband two-photon absorption (TPA).

Figure 2A depicts a schematic illustration of potential exciton transitions across energy states in a quantum dot system after valence band states have been mixed [11]. Single photon absorption can happen after $1S_e - 1(S, D)_{3/2}$, representing $E_g$, $1S_e - 2(S, D)_{3/2}$ and $1P_e - 1(P, F)_{3/2}$ in our experimental setup. While following $1S_e - 1P_{3/2}$ and $1P_e - 1S_{3/2}$ transitions, two-photon absorption is possible [12]. We utilised a spectroscopic model [13] that accounts for both intra-band ESA and 2PA to quantify several causes causing the observed drop in transmittance at higher intensities. All of these NCs exhibit bi-exponential decays, which indicate a faster and a slower component, in the radiative (photoluminescence (PL) decay) lifetimes that have been calculated by making the use of the time correlation single photon counting (TCSPC) approach (Table 1). All potential single-photon interband exciton transition contributions, including the HOMO and LUMO contributions, have been assumed to originate from the single state $|1\rangle$ with a cross-section of $\sigma_1$. Similar to this, it is believed that $|2\rangle$ with a cross-section $\sigma_{ex}$ is the source of all intraband transitions LUMO electron states ($1p_e$ and above represented by state $|n\rangle$ leading to ESA. The symbols $\tau_1$ and $\tau_2$ denote, respectively, the nonradiative relaxation periods from the higher electron states to LUMO and the radiative recombination times (PL decay times) of the excited carriers. As previously mentioned, a simple quantitative model is shown in Figure 2B.

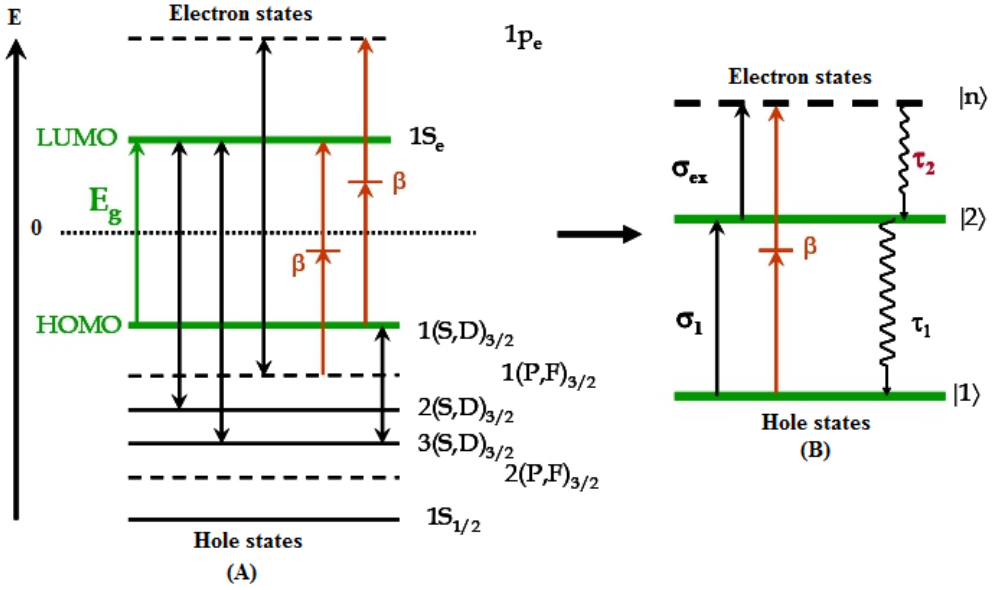


**Figure 2:** Diagram showing (A) potential exciton transitions in a QD system taking valence band state mixing into account and (B) a simplified model to quantify the processes.

The rate equations may be expressed by denoting the population at level $|i\rangle$ by $n_i$:

$$\frac{dn_1}{dt} = -\frac{\sigma_1 I n_1}{h\nu} - \frac{\beta I^2}{2h\nu} + \frac{n_2}{\tau_1} \quad (1)$$

$$\frac{dn_2}{dt} = \frac{\sigma_2 I n_1}{h\nu} - \frac{\sigma_{ex} I n_2}{h\nu} - \frac{n_2}{\tau_1} + \frac{n_n}{\tau_2} \quad (2)$$

$$\frac{dn_n}{dt} = \frac{\sigma_{ex} I n_2}{h\nu} + \frac{\beta I^2}{2h\nu} - \frac{n_n}{\tau_2} \quad (3)$$

and the sample's intensity transmission is determined by

$$\frac{dI}{dz} = -\sigma_1 I n_1 - \sigma_{ex} I n_2 - \beta I^2 \quad (4)$$

where $h\nu$ stands for energy of the excitation photon and equal to total two-photon absorption coefficient from the transitions $1P_e - 1(S, D)_{3/2}$ and $1S_e - 1(P, F)_{3/2}$. I represents the intensity of the Gaussian beam in terms of *r*, *t*, and *z*. A least square fitting of experimental data is used to solve the differential equations numerically to yield $\sigma_{ex}$, $\beta$ and $\tau_2$ [7, 8]. The equation $\sigma_{2PA} = (h\nu/n_1)\times\beta$, where $n_1$ is the dot number density in the solution, have been utilized in the determination of two-photon absorption cross-section [14].

**Table 1:** TNC and QNC sizes, band gaps, and two-photon cross-sections in heptanes.

| Quantum dots | Estimated size by TEM (nm) | Energy gap (eV) | PL decay ($\tau_1$) (ns) | two-photon absorption cross-section ($\times 10^{-48}$ $cm^4$s/photon) |
|---|---|---|---|---|
| CdSeS-I | 6.2 | 2.05 | 1.2, 18.6 | 3.87 |
| CdSeS-II | 6.2 | 2.26 | 1.4, 16.9 | 3.79 |
| ZnCdSeS-I | 6.4 | 2.1 | 0.36, 6.2 | 13.92 |
| ZnCdSeS-II | 6.7 | 2.0 | ------ | 19.23 |

We deduced from the theoretical fits that the mechanism causing the observed drop in transmittance near focus is two-photon absorption. Whereas TNCs with band gap energies equal to 2.26 and 2.05 eV respectively exhibit two-photon absorption cross-sections ($\sigma_2$) of 3.79 and $3.87\times10^{-48}$ $cm^4$s/photon, respectively, it was discovered that QNCs have an order larger 2 than their ternary counterparts (Table 1). The nonradiative relaxation periods $\tau_2$ discovered from the fit agrees well with the earlier observations [15] and range from a few hundred fs ( 500 fs) to a few ps (1 - 6 ps) in length. Although the observed $\sigma_{2PA}$ is comparable to that of CdS NCs, the onset of TPA under resonant excitation conditions has started off at relatively lower peak intensities than in previous reports with picosecond [16] and femtosecond lasers [17], indicating the presence of stronger nonlinearity in these NCs. Even at very low input intensities, these materials exhibit exclusively RSA behaviour with 1064 nm excitation because of two-photon absorption having the cross-section of the order of $10^{-47}$ $cm^4$s/photon. A highly strong excitonic transition that is available for two-photon absorption is indicated by the occurrence of such a high $\sigma_{2PA}$ at low input intensity.

## 4. Conclusions

We investigated innovative gradient-structured ternary and quaternary semiconductor NCs in the ps regime under both resonant and nonresonant electronic excitation circumstances. We can clearly identify the beginning of the intensity-dependent absorption process in these NCs and precisely detect the initiation of RSA caused by two-photon absorption in picosecond time scales. We can also separate the mechanisms occurring at various input intensity levels. At increasing input intensity, the nonlinear absorption behaviour under resonant excitation transitions from SA to an appearance of RSA, showing an intensity-dependent two-photon absorption channel. These colloidal NCs are suitable candidates for two-photon absorption dependent picosecond optical limiters due to beginning of the RSA at lower intensities achieved by adjusting the bandgap energy and a very good two-photon absorption at lower intensities under nonresonant stimulation.

## References


[1] M.A. El-Sayed, Small is different: Shape-, size-, and composition-dependent properties of some colloidal semiconductor nanocrystals, *Acc. Chem. Res.* **37** (2004) 326 – 333.

[2] G.P. Banfi, V. Degiorgio, D. Ricard, Nonlinear optical properties of semiconductor nanocrystals, *Adv. Phys.* **47** (1998) 447–510.

[3] G. Konstantatos, I. Howard, A. Fischer, S. Hoofland, J. Clifford, E. Klem, L. Levina, E.H. Sargent, Ultrasensitive solution-cast quantum dot photodetectors, *Nature* **442** (2006) 180–183.

[4] N. Peyghmbarian, B. Fluegel. D. Hulin, A. Migus, M. Joffre, A. Antonetti, S.W. Koch, M. Lindberg, Femtosecond optical nonlinearities of CdSe quantum dots, *IEEE J. Quantum Electron.* **25** (1989) 2516 – 2522.

[5] J. He, W. Ji, G.H. Ma, S.H. Tang, H.I. Elim, W.X. Sun, Z.H. Zhang, W.S. Chin, Excitonic nonlinear absorption in CdSnanocrystals studied using Z-scan technique, *J. Appl. Phys.* **95** (2004) 6381 – 6386.

[6] X. Wang, Y. Du, S. Ding, Q. Wang, G. Xiang, M. Xie, X. Chen, D. Peng, Preparation and third-order optical nonlinearity of self-assembled chitosan/CdSe–ZnS core–shell quantum dots multilayer films, *J. Phys. Chem.* B **110** (2006) 1566 – 1570.

[7] P.P. Kiran, D.R. Reddy, B.G. Maiya, A.K. Dharmadhikari, G.R. Kumar, D.N. Rao, Nonlinear absorption properties of axial-bonding type tin(IV) tetratolyporphyrin based hybrid porphyrin arrays, *Opt. Commun*. **252** (2005) 150 – 161.

[8] N.K.M.N Srinivas, S.V. Rao, D.N. Rao, Saturable and reverse saturable absorption of rhodamine b in methanol and water, *J. Opt. Soc. Am. B*. **20** (2003) 2470 – 2479.

[9] M. Jung, J. Lee, J. Park, J. Koo, Y. M. Jhon, and J. H. Lee, Mode-locked, 1.94-μm, all-fiberized laser using WS2-based evanescent field interaction, *Opt. Express* **23** (2015) 19996–20006.

[10] M. Sheik-Bahae, A.A. Said, T-H. Wei, D.J. Hagan, E.W. Vanstryland, Sensitive measurement of optical nonlinearities using a single beam, *IEEE J. Quantum Electron.* **16** (1990) 760 – 769.

[11] U. Woggon, *Energy States,* in Optical Properties of Semiconductor Quantum Dots, Springer Tracts in Modern Physics, Springer (1996).

[12] S.V. Gaponenko, *Resonant optical nonlinearites and related many-body effects,* in Optical Properties of Semiconductor Nanocrystals, Cambridge University Press, USA (1998).

[13] V.G. Savitski, A.M. Malyarevich, M.I. Demchuk, K.V. Yumashev, H. Raaben, A.A. Zhilin, Intensity-dependent bleaching relaxation in lead salt quantum dots, *J. Opt. Soc. Am. B.* **22** (2005) 1660 – 1666.

[14] G.S. He, J.D. Bhawalkar, C.F. Zhao, P.N. Prasad, Optical limiting effect in a two-photon absorption dye doped solid matrix, *Appl. Phys. Lett.* **67** (1995) 2433 – 2435.

[15] V.I. Klimov, Optical nonlinearities and ultrafast carrier dynamics in semiconductor nanocrystals *J. Phys. Chem. B*. **104** (2000) 6112 – 6123.

[16] M.Y. Han, W. Huang, C.H. Chew, L.M. Gan, X.J. Zhang, W. Ji, Large nonlinear absorption in coated $Ag_2S$/CdS nanoparticles by inverse microemulsion, *J. Phys. Chem. B* **102** (1998) 1884 – 1887.

[17] J. He, J. Mi, H. Li, W. Ji, Observation of interband two-photon absorption saturation in CdS nanocrystals, *J. Phys. Chem. B* **109** (2005) 19184 –19187.